Supplementary information

Solvent Free Depolymerization of Kraft lignin to Alkyl-phenolics using Supported NiMo and CoMo Catalysts

Chowdari Ramesh Kumar[a], Narani Anand[b], Arjan Kloekhorst[a], Catia Cannilla[c],

Giuseppe Bonura[c], Francesco Frusteri[c], Katalin Barta[b,*], Hero Jan Heeres[b,*]

[a]*Chemical Engineering Department, Faculty of Mathematics and Natural Science,*

University of Groningen, Nijenborgh 4, 9747 AG Groningen, The Netherlands

[b]*Stratingh Institute of Chemistry, Faculty of Mathematics and Natural Science,*

University of Groningen, Nijenborgh 4, 9747 AG Groningen, The Netherlands

[c]*CNR-ITAE, Istituto di Tecnologie Avanzate per l'Energia "Nicola Giordano"*

Via S. Lucia sopra Contesse, 5 – 98126 Messina, Italy

1. Catalyst characterization techniques

TPD of NH₃ and CO₂. Surface concentrations of acidic and basic sites were determined by temperature programmed desorption of ammonia (NH_3-TPD) and carbon dioxide (CO_2-TPD), respectively. Before TPD experiments, the catalysts (~50 mg) were reduced, at atmospheric pressure, by flowing hydrogen (60 *STP* ml/min) in a linear quartz micro-reactor (*l*, 200 mm; *i.d.*, 4mm) from room temperature to 500 °C at a heating rate of 10 °C/min. Then, the samples were maintained under hydrogen flow at 500 °C for 30 min. After cleaning with helium, the samples were saturated for 60 min in flow of a gas mixture containing 5 vol.% of NH_3/He at 150°C or alternatively 10 vol.% of CO_2 at 200 °C. In both cases the total flow rate was 25 ml/min. Then, the samples were purged in helium flow until a constant baseline level was attained. TPD measurements were performed in the temperature range 100–600 °C at a rate of 10 °C/min using helium (25 *STP* ml/min) as carrier flow. The evolved ammonia or carbon dioxide were detected by an on-line thermal-conductivity detector, calibrated by the peak area of known pulses of NH_3 or CO_2.

XRD. Powdered samples were analyzed by using a Philips X-Pert Diffractometer, operating with a Ni *β*-filtered Cu K*α* radiation (λ=1.5406 Å) at 40 kV and 30 mA. Data were collected over a 2*θ* range of 10-100 degree, with a step size of 0.04° at a time per step of 3s.

BET. Surface area, pore volume and pore size distribution were determined from the nitrogen adsorption/desorption isotherms at −196 °C, using a Micromeritics' ASAP2020 Instruments gas adsorption device. Before analysis, all samples were out gassed at 180 °C under vacuum for 5 h. Only the carbon containing samples were out gassed at 180 °C for 12 h.

FT-IR. Fourier Transform Infrared spectra were acquired on a FT-IR (Spectrum 2000, Perkin-Elmer, UK) ATR (attenuated total reflectance) golden gate apparatus (Graseby-Specas Ltd., Orpington, UK). A total of 16 scans with a resolution of 4 cm^{-1} were measured.

2. Analytical techniques

The gas phases were collected after reaction and stored in a gas bag (SKC Tedlar 3 L sample bag (9.5"×10")) with a polypropylene septum fitting. GC-TCD analyses were performed using a Hewlett Packard 5890 Series II GC equipped with a Porablot Q Al_2O_3/Na_2SO_4 column and a molecular sieve (5 A) column. The injector temperature was set at 150 °C and the detector temperature at 90 °C. The oven temperature was kept at 40 °C for 2 minutes then heated up to 90 °C at 20 °C min^{-1} and kept at this temperature for 2 minutes. A reference gas was used to quantify the results (55.19% H_2, 19.70% CH_4, 3.00% CO, 18.10% CO_2, 0.51% ethylene, 1.49% ethane, 0.51% propylene and 1.5% propane). The reference gas was used to identify the peaks by retention time and to quantify the amounts.

DCM soluble products were analysed by GC-MS-FID using a Quadruple Hewlett Packard 6890 MSD attached to a Hewlett Packard 5890 GC equipped with a sol-gel capillary column (60 m × 0.25 mm i.d. and a 0.25 μm). The injector temperature was set at 250 °C. The oven temperature was kept at 40 °C for 5 minutes, then heated to 250 °C at a rate of 3 °C min^{-1} and then held at 250 °C for 10 minutes.

GC×GC-FID analysis was performed on the organic samples using a trace GCxGC from Interscience equipped with a cryogenic trap system and two columns (a 30 m × 0.25 mm i.d. and a 0.25 μm film of RTX-1701 capillary column connected by a meltfit to a 120 cm × 0.15 mm i.d. and a 0.15 μm film Rxi-5Sil MS column). An FID detector was used. A dual jet modulator was applied using carbon dioxide to trap the samples. Helium was used as the carrier gas (continuous

flow 0.6 ml min^{-1}). The injector temperature and FID temperature were set at 250 °C. The oven temperature was kept at 40 °C for 5 minutes and then heated up to 250 °C at a rate of 3 °C min^{-1}. The pressure was set at 70 kPa at 40 °C. The modulation time was 6 seconds.

For GCxGC-FID and GC-MS-FID analyses, the samples were diluted with tetrahydrofuran (THF) and 500 ppm di-n-butyl ether (DBE) was added as an internal standard. GPC analyses of the samples were performed using a HP1100 equipped with three MIXED-E columns (300 × 7.5 mm PL gel 3 μm) in series using a GBC LC 1240 RI detector. Average molecular weight calculations were performed using the PSS WinGPC Unity software from Polymer Standards Service. The following conditions were used: THF as the eluent at a flow rate of 1 ml min^{-1}; 140 bar, a column temperature of 40 °C, 20 μl injection volume and a 10 mg ml^{-1} sample concentration. Toluene was used as a flow marker. The GCxGC-FID calibration procedure is as follows:

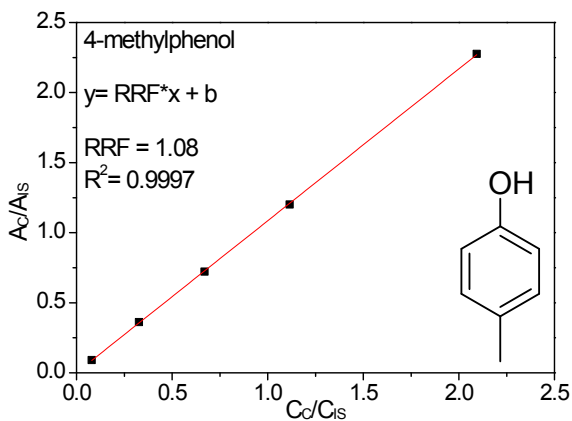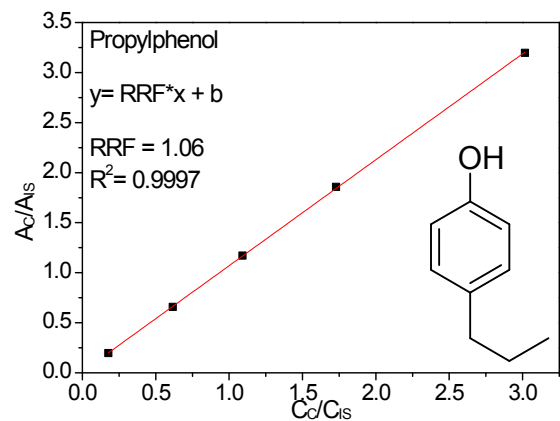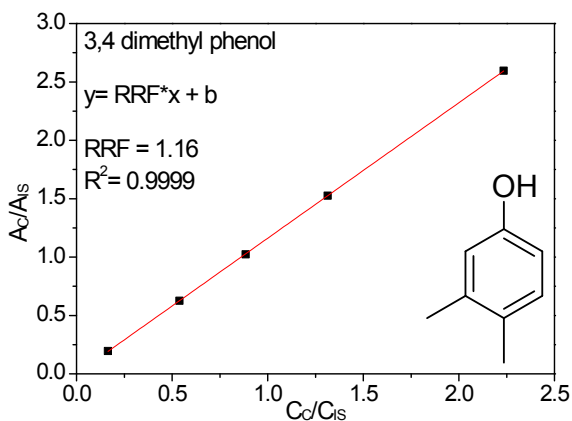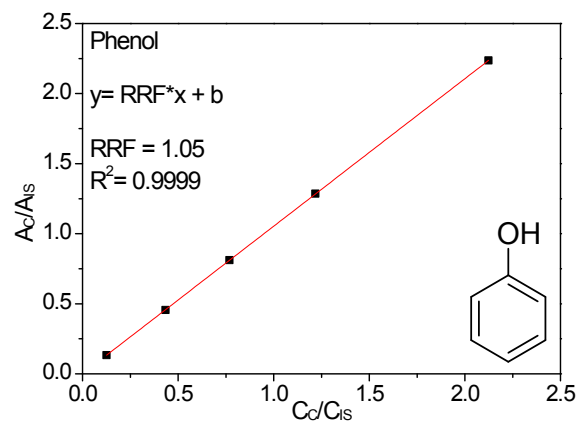## 2.1 Calibration of GC×GC-FID chromatograms

The first step in the quantification procedure involved determination of the RRF value for a number of representative model components belonging to the various compound groups (alkylphenolics, aliphatic hydrocarbons, aromatics,). The following equation was used to calculate the RRF for an individual model component:
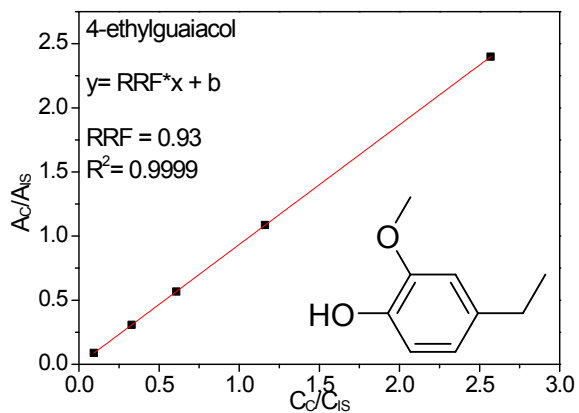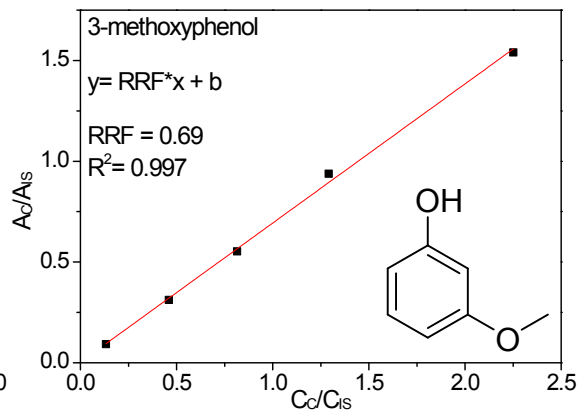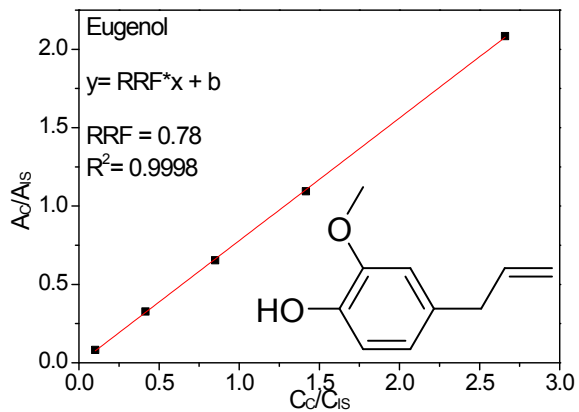
$$RRF = \frac{C_{IS}.A_c}{C_c.A_{IS}}$$

Where C_{IS} is the concentration of the internal standard, A_{IS} the area of the internal standard (di-n-butylether,DBE), C_C the concentration of the component C, A_C is the area of the component, and RRF is the relative response factor for compound C.

The RRF value for an individual model component was determined by plotting the ratio C_c/C_{IS} versus the ratio A_c/A_{IS}. In such a plot, (see below), the slope is the RRF value for the individual model component.
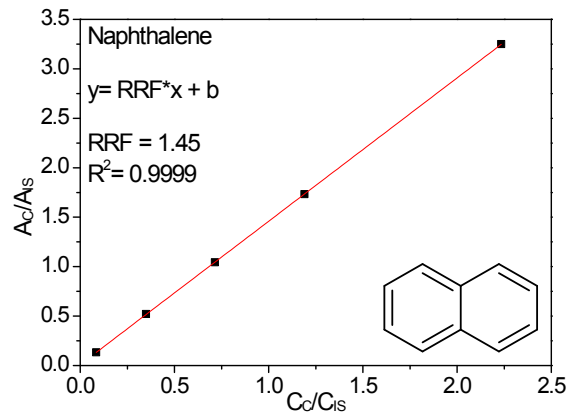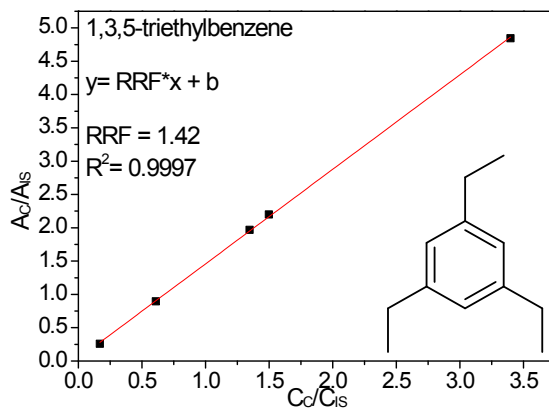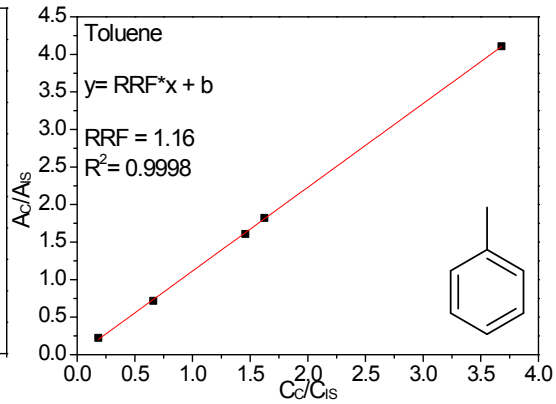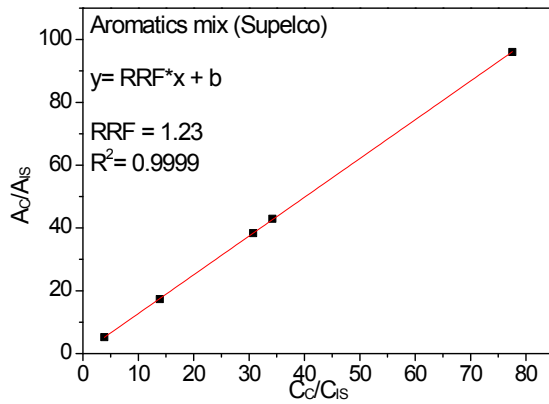
Examples for the (alkylated) phenolic group:

Examples for the alkylated methoxy phenolics:

Eugenol

y= RRF*x + b

RRF = 0.78
R^2= 0.9998

(A_C/A_{IS} vs C_C/C_{IS})

3-methoxyphenol

y= RRF*x + b

RRF = 0.69
R^2= 0.997

(A_C/A_{IS} vs C_C/C_{IS})

4-ethylguaiacol

y= RRF*x + b

RRF = 0.93
R^2= 0.9999

(A_C/A_{IS} vs C_C/C_{IS})

Examples for the aromatics:

For the quantification based on compound groups, the total compound group area was calibrated over a concentration range of 10 to 100 mg/kg by using 5 calibration mixtures. From these calibrations, an average RRF is calculated for each compound group, see Table below.

Compound group	RRF (DBE)
Alkylated phenolics	1.1
Methoxylated alkylated phenolics	0.9
Aromatics/Naphthalenes	1.23
Linear/branched alkanes	1.6
Cyclic alkanes	1.5
Ketones/Alcohols	1

^{13}C NMR spectra were acquired at 25 °C using an Agilent 400 MHz spectrometer. Approximately 0.1 g of DCM soluble product/Kraft lignin was dissolved in 0.6 ml dimethylsulfoxide-d6 (DMSO). The number of scans was 2048 with a relaxation time of 5 sec. The data were processed using the MestReNova software.

Elemental analyses (C, H, N and S) were performed using a Euro Vector 3400 CHN-S analyzer. The oxygen content was determined by difference. All experiments were carried out in duplicate and the average value is provided.

3. X-ray diffraction patterns

The formation of the $NiMoO_4$/$CoMoO_4$ phase was clearly detected by powder XRD, for the NiMo/AC and CoMo/AC catalysts.[1,2] For all the other supports, the diffraction signals of the support were more dominant, covering the peaks arising from NiMoO4 or CoMoO4 phases. This indicates a good distribution of the active component on the amorphous support. The corresponding diffraction patters are shown in Figure S1.
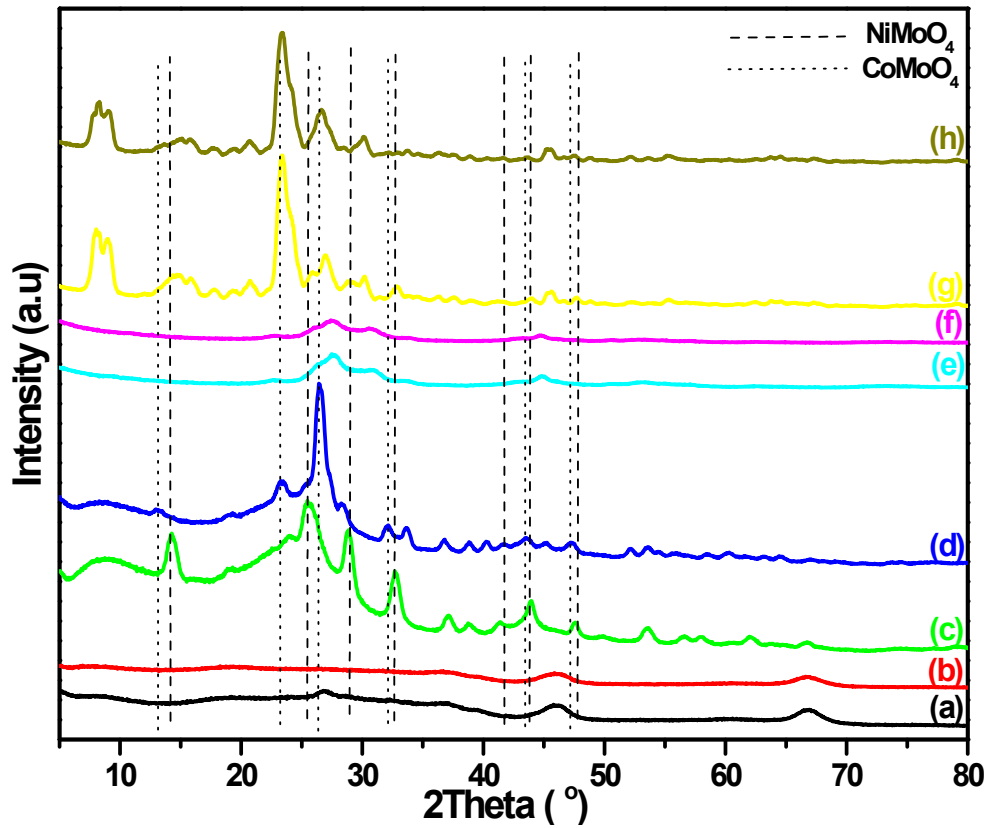
Fig. S1 XRD patterns of (a) NiMo/Al₂O₃, (b) CoMo/Al₂O₃, (c) NiMo/AC, (d) CoMo/AC, (e) NiMo/MgO-La₂O₃, (f) CoMo/MgO-La₂O₃, (g) NiMo/ZSM-5, and (f) CoMo/ZSM-5.

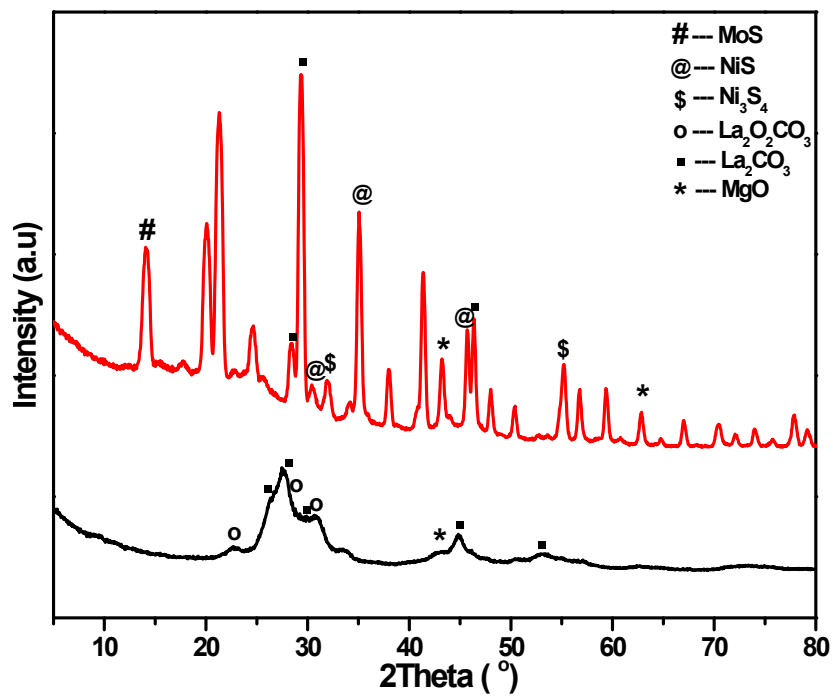**Fig. S2** XRD patterns of NiMo/MgO-La$_2$O$_3$ (fresh) and S-NiMo/MgO-La$_2$O$_3$ (used) catalysts.
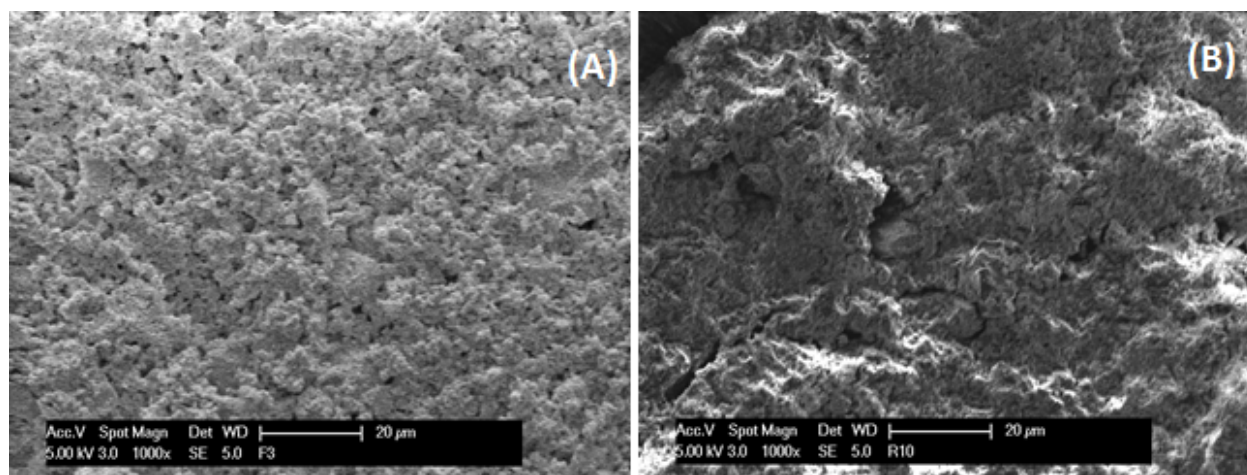
Fig. S3 SEM images of (A) "fresh" NiMo/MgO-La$_2$O$_3$ catalyst and (B) "used" S-NiMo/MgO-La$_2$O$_3$ catalyst.
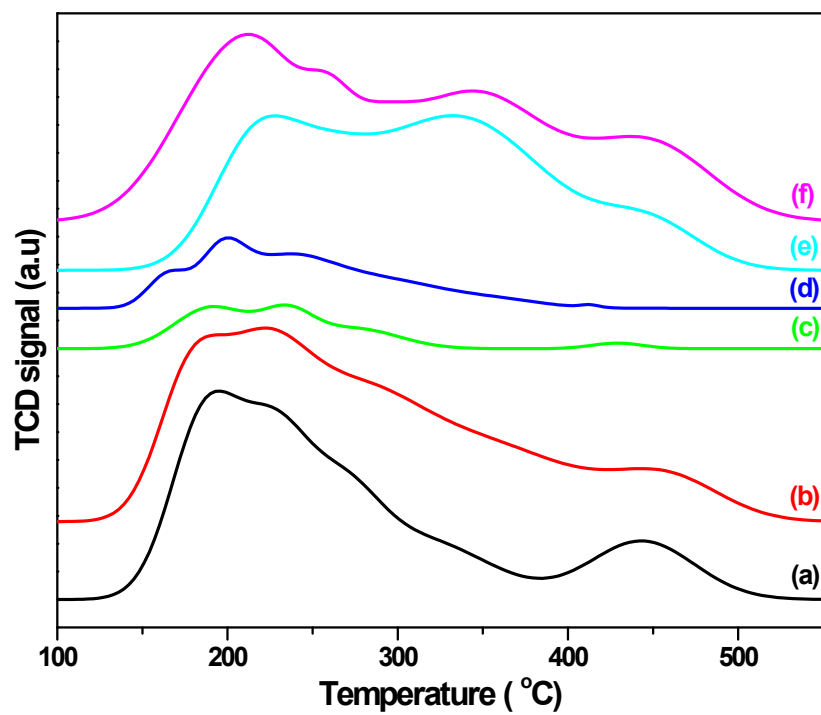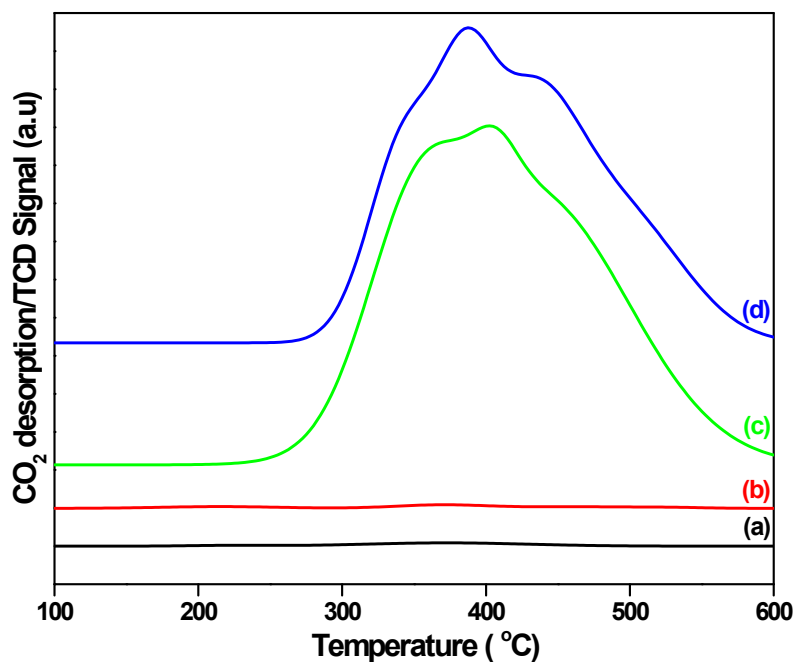
Fig. S4 Temperature programmed desorption of ammonia patterns: (a) NiMo/Al$_2$O$_3$; (b) CoMo/Al$_2$O$_3$; (c) NiMo/AC; (d) CoMo/AC; (e) NiMo/ZSM-5 and (f) CoMo/ZSM-5.

Fig. S5 Temperature programmed desorption of CO_2 patterns of (a) NiMo/AC; (b) CoMo/AC; (c) NiMo/MgO-La_2O_3; (d) CoMo/MgO-La_2O_3.
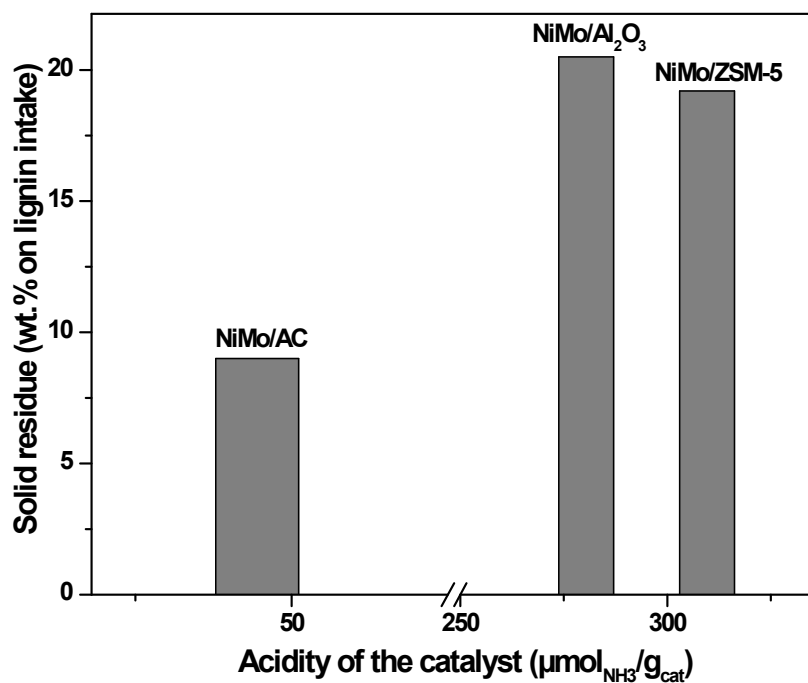

Fig. S6 The relation between formation of the solid residue and acidity of the NiMo supported on AC, ZSM-5, Al_2O_3.
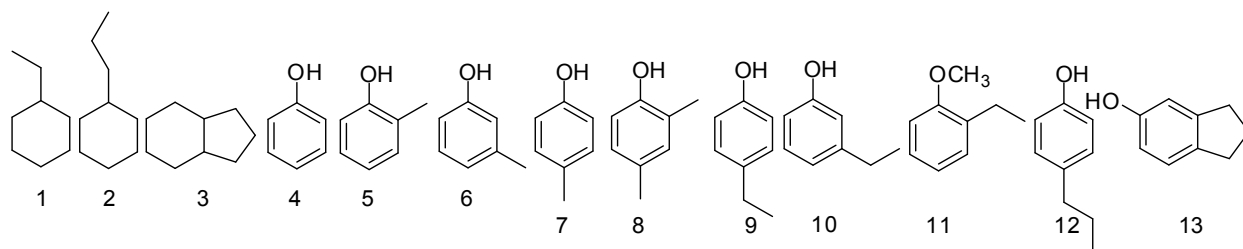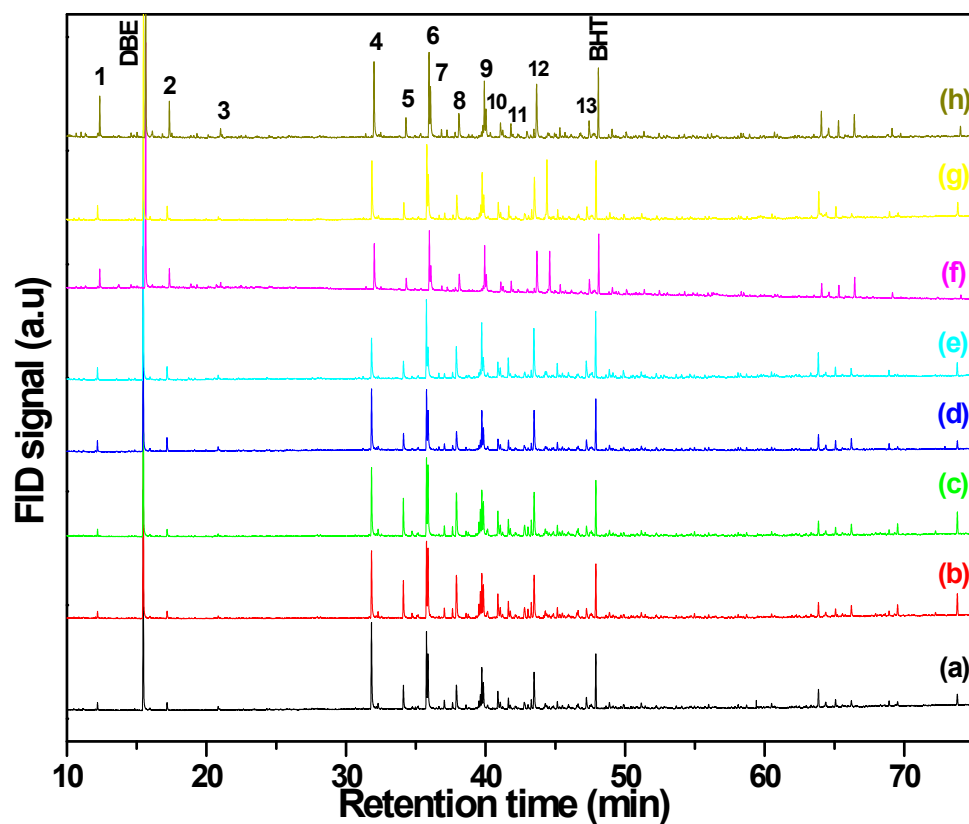
Fig. S7 GC-MS-FID chromatograms of lignin oil obtained among various catalysts: (a) S-NiMo/Al₂O₃; (b) S-CoMo/Al₂O₃; (c) S-NiMo/AC; (d) S-CoMo/AC; (e) S-NiMo/MgO-La₂O₃; (f) S-CoMo/MgO-La₂O₃; (g) S-NiMo/ZSM-5 and (f) S-CoMo/ZSM-5.

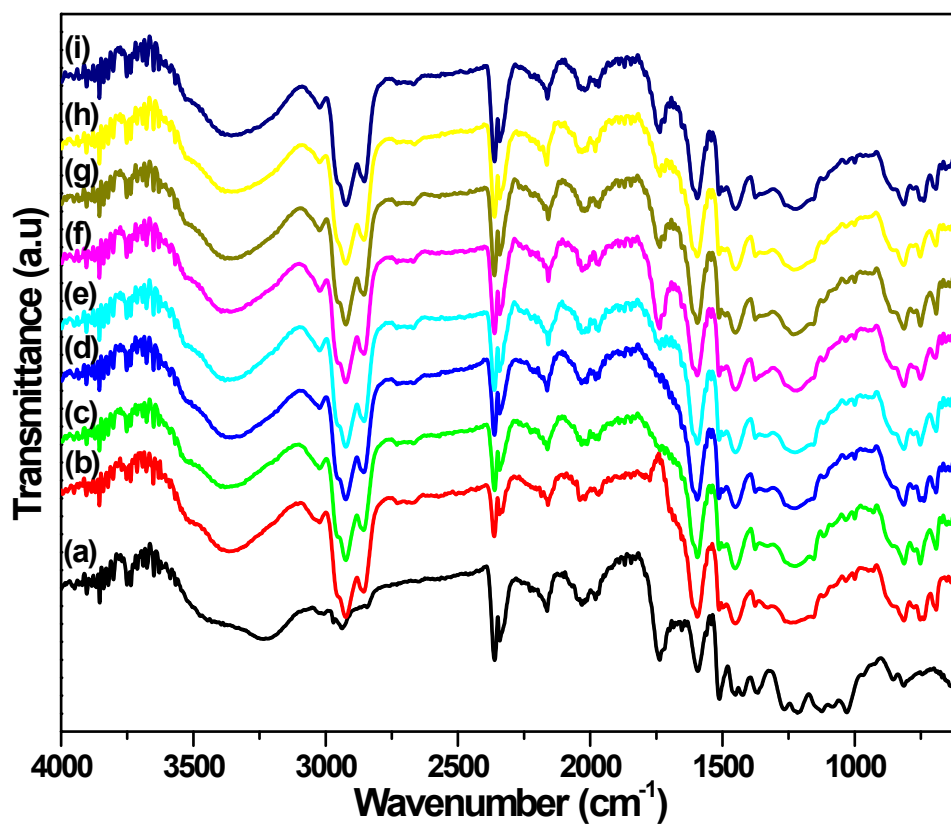**Fig. S8** FT-IR spectra of Kraft lignin and lignin oils obtained among various catalysts: (a) Kraft lignin; (b) S-NiMo/Al$_2$O$_3$; (c) S-CoMo/Al$_2$O$_3$; (d) S-NiMo/AC; (e) S-CoMo/AC; (f) S-NiMo/MgO-La$_2$O$_3$; (g) S-CoMo/MgO-La$_2$O$_3$; (h) S-NiMo/ZSM-5 and (i) S-CoMo/ZSM-5.
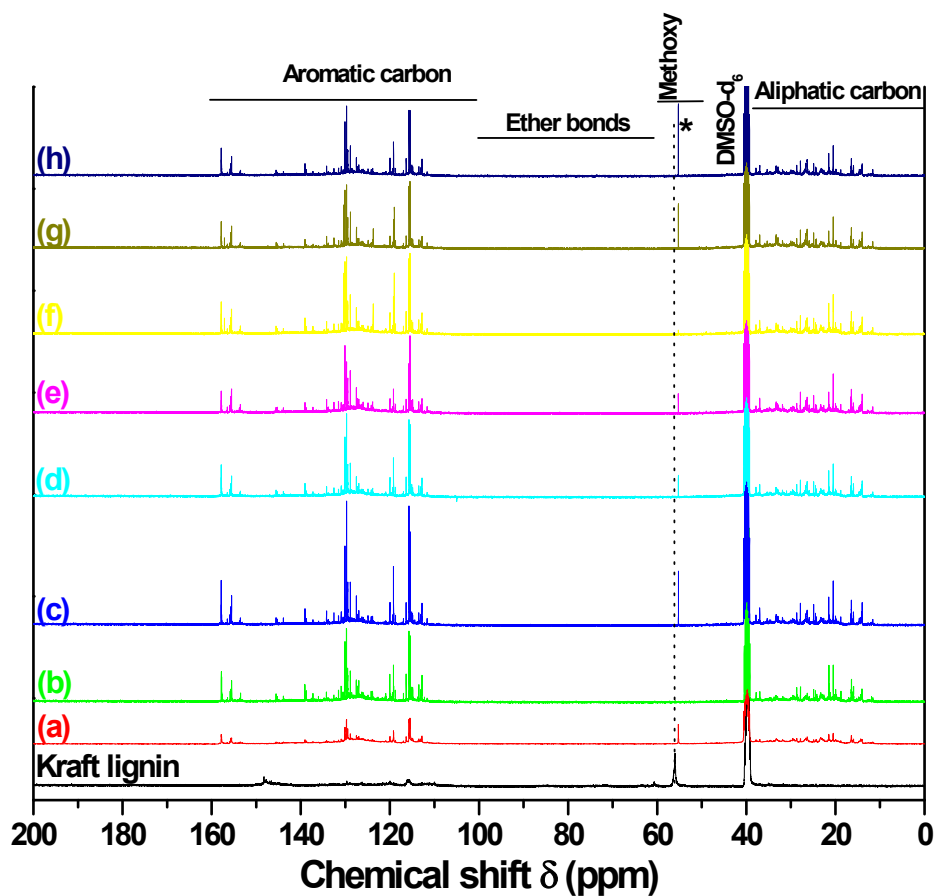
Fig. S9 ^{13}C-NMR spectra of Kraft lignin and DSPs obtained over various catalysts: (a) S-NiMo/Al$_2$O$_3$; (b) S-CoMo/Al$_2$O$_3$; (c) S-NiMo/AC; (d) S-CoMo/AC; (e) S-NiMo/MgO-La$_2$O$_3$; (f) S-CoMo/MgO-La$_2$O$_3$; (g) S-NiMo/ZSM-5 and (f) S-CoMo/ZSM-5.

Table S1 Textural properties of the catalysts.

Catalyst	BET surface area $(m^2 g^{-1})$	Pore volume $(cm^3 g^{-1})$	Particle size* (nm)
NiMo/MgO-La$_2$O$_3$ (fresh)	29.5	0.16	4.3
S-NiMo/MgO-La$_2$O$_3$ (used)	23.1	0.14	15.7

* Particle size calculated from the XRD, using the Scherrer equation.

Table S2 Average molecular weights and polydispersity indexes for DSPs and ASPs.

Catalyst	DSP- M_w	ASP- M_w
S-NiMo/Al$_2$O$_3$	620	1280
S-CoMo/Al$_2$O$_3$	480	950
S-NiMo/AC	750	2180
S-CoMo/AC	670	1910
S-NiMo/MgO-La$_2$O$_3$	660	1580
S-CoMo/MgO-La$_2$O$_3$	890	2380
S-NiMo/ZSM-5	620	1500
S-CoMo/ZSM-5	760	2010

Table S3 Elemental analysis of lignin depolymerized products.

Lignin oil	DSPs			ASPs		
	C %	H %	O %	C%	H%	O%
S-NiMo/Al$_2$O$_3$	82.9	7.7	8.4	79.1	6.1	13.2
S-CoMo/Al$_2$O$_3$	84.8	7.9	6.4	81.9	6.7	9.8
S-NiMo/AC	82.5	7.9	8.9	80.1	6.5	11.7
S-CoMo/AC	83.6	7.9	7.5	80.2	6.5	11.6
S-NiMo/MgO-La$_2$O$_3$	83.8	7.9	7.1	80.2	6.3	11.5
S-CoMo/MgO-La$_2$O$_3$	84.3	7.8	6.7	81.5	6.8	9.8
S-NiMo/ZSM-5	83.4	8.2	7.3	80.8	6.3	11.1
S-CoMo/ZSM-5	84.3	8.2	6.5	80.8	6.5	10.9

Reference:

1   E.T. Liakakou, E. Heracleous, K.S. Triantafyllidis and A.A. Lemonidou, *Appl. Catal. B*, 2015, **165**, 296.

2   T. Yang, H. Zhang, Y. Luo, L. Mei, D. Guo, Q. Li and T. Wang, *Electrochim. Acta*, 2015, **158**, 327.